

# Grapefruit Seed Extract and Lemon Essential Oil as Active Agents in Corn Starch–Chitosan Blend Films

M. J. Bof<sup>1</sup> · A. Jiménez<sup>2</sup> · D. E. Locaso<sup>1</sup> · M. A. García<sup>3</sup>  · A. Chiralt<sup>2</sup>

Received: 11 March 2016 / Accepted: 5 August 2016 / Published online: 13 August 2016  
© Springer Science+Business Media New York 2016

**Abstract** The effect of lemon essential oil (LEO) and grapefruit seed extract (GSE) addition to starch–chitosan blend films on their functional properties and the associated structural changes were studied. Likewise, the films' antioxidant properties and antimicrobial activity against some molds and Gram (+) and Gram (–) bacteria was evaluated. Composite active films exhibited a yellowish color, especially in the case of LEO addition. Film microstructure was analyzed by SEM evidencing a good incorporation of GSE to film matrix, while LEO droplets were dispersed in the polymer blend. Oxygen and water vapor barrier properties were not notably modified by the presence of active agents. FTIR analyses revealed that hydrogen bonding occurs in the blend films as the main interaction mechanism between components. Films containing LEO or GSE were less stiff and resistant but more stretchable than the control ones, being this effect concentration dependent. No notable antimicrobial action was observed in the films, which suggest that the required final concentration of active compounds must be fitted considering the minimum inhibitory concentration (MIC) values for a specific microorganism and its release kinetics to the food matrix.

**Keywords** Starch–chitosan films · Lemon essential oil · Grapefruit seeds extract antimicrobials · Tensile and barrier properties

## Introduction

Nowadays, consumers are demanding environmentally friendly and biodegradable packaging materials as well as a reduction in the use of chemicals as food preservatives (Han 2014). In this sense, polymers obtained from renewable and natural sources are being widely investigated for food and pharmaceutical applications due to their biodegradability and greater biocompatibility as compared to those based on petroleum-derived polymers. In the field of food production in particular, the application of edible films offers a promising alternative to reduce the use of conventional packaging in order to improve food preservation and decay control and lessen the negative impact of plastic waste.

There are different available polymers that can be used to obtain biodegradable films. Of these, corn starch is one of the most widely used polymers due to its well-known good film-forming capacity, low cost, biodegradability, availability, and good barrier properties to gases (CO<sub>2</sub> and O<sub>2</sub>) (Bertuzzi et al. 2007; De Campos et al. 2011). On the other hand, chitosan, a polymer obtained by deacetylation of chitin commonly extracted from crab shells, presents particular interest due to its inherent antimicrobial activity against some microorganisms (No et al. 2002). The antimicrobial properties of chitosan derive from its polycationic nature. Its mode of action is attributed to the formation of electrostatic bounds between the protonated amino groups of chitosan and the negative residues of the cell wall surface (Tsai et al. 2002). This activity against microorganisms depends on some specific

---

✉ M. A. García  
magarcia@quimica.unlp.edu.ar

<sup>1</sup> Facultad de Ciencias de la Alimentación, Universidad Nacional de Entre Ríos, Monseñor Tavella 1450, 3200 Concordia, Entre Ríos, Argentina

<sup>2</sup> Instituto de Ingeniería de Alimentos para el Desarrollo, Universitat Politècnica de València, Camino de Vera s/n, 46022 Valencia, Spain

<sup>3</sup> Centro de Investigación y Desarrollo en Criotecnología de Alimentos (CIDCA), Facultad Ciencias Exactas, Universidad Nacional de La Plata, 47 y 116 S/N, La Plata (B1900AJJ), Buenos Aires, Argentina

characteristics of the polymer, such as deacetylation degree (DD) and molecular weight (MW) (Liu et al. 2002). Chitosan also exhibits good film-forming capacity and it has been widely studied in this sense (Sanchez-Gonzalez et al. 2010). Due to its hydrophilic nature, chitosan films exhibit poor water vapor barrier properties and they are highly water sensitive (Vargas et al. 2012).

Some authors have studied the properties of blend films with different proportions of chitosan and starch from different sources (Bonilla et al. 2013; García et al. 2006; Mei et al. 2013; Bof et al. 2014, 2015). Starch–chitosan blend films exhibited improved tensile properties with respect to pure polymer films while chitosan imparts antimicrobial properties to the blend films.

Likewise, to enhance the antibacterial and antioxidant properties of chitosan, other antimicrobials could be incorporated to achieve a synergistic effect. In this sense, essential oils and extracts obtained from plants have been incorporated in formulations for antimicrobial or antioxidant purposes (Boumail et al. 2013; Hosseini et al. 2016). Lemon essential oil (LEO) and grapefruit seed extract (GSE) can be obtained as byproducts from citric processing and are natural additives that could be used in food preservation. Nevertheless, the chemical composition of plant essential oils may vary according to species, part of the plant, season of harvesting, and geographical origin (Teixeira et al. 2013). In addition, the extraction method can also influence the type and amount of extracted molecules. The main component of lemon essential oils is  $\alpha$ -limonene, followed by  $\alpha$ - and  $\beta$ -pinene,  $\alpha$ -terpineol,  $\beta$ -myrcene,  $\alpha$ -terpinolene, terpinen-4-ol, cymene and, in a minor proportion,  $\epsilon$ -citralin (AL-Jabri and Hossain 2014). Grapefruit seed extract contains large quantities of polyphenolic compounds, such as catechins; epicatechin; epicatechin-3-O-gallate; and dimeric, trimeric and tetrameric procyanidins (Xu et al. 2007a). Likewise, the beneficial actions of GSE have partly been attributed to the antioxidant activity of citrus flavonoids, such as naringenin (Xu et al. 2007a).

The effect of lemon essential oil and grapefruit seed extract on the microorganisms' growth has been studied, and their efficiency against molds has been reported (Xu et al. 2007b). However, there is no available information about either their action when included in chitosan–corn starch blend films or their effect on the functional properties of the composite polymer matrix.

The aim of this work was to analyze the effect of the incorporation of LEO and GSE in starch–chitosan blend films on their functional (tensile, barrier, and optical) properties, associated with the structural changes provoked in the polymer matrix, and to evaluate the films' antioxidant properties and antimicrobial activity against some molds and Gram (+) and Gram (–) bacteria.

## Materials and Methods

### Materials

Chitosan powder (Parafarm, Buenos Aires, Argentine) with medium molecular weight (444 kDa; Bof et al. 2015) and corn starch (Glutal, Buenos Aires, Argentine) containing 25 % amylose were used for film matrix development. Lemon essential oil (LEO) was obtained from Litoral Citrus (Buenos Aires, Argentine) and grapefruit seed extract (GSE) (7.52 % solids content) was provided by Euma (Euma SAICI y F, Buenos Aires, Argentine), both stored in a dark container at 4 °C until use. Glycerol, used as plasticizer, was supplied by Panreac Química S.A. (Castellar del Vallès, Barcelona, Spain).

### Preparation of Film-Forming Dispersion

A 4 % (w/w) corn starch aqueous suspension (CS) was prepared, which was then gelatinized for 20 min at 85 °C. Furthermore, chitosan (CH) powder was dissolved in 1.25 % (w/w) acetic acid in order to obtain 2.5 % (w/w) chitosan solutions, under stirring for 24 h. Then, it was filtered through a screen (400  $\mu$ m mesh) to remove impurities.

In order to obtain the film-forming dispersions (FFDs), CS and CH were mixed in a proportion of 75:25 (w/w), on the basis of previous studies (Bof et al. 2014). LEO or GSE were incorporated in order to obtain 1 and 3 % w/w in the FFD. The concentrations used were similar to those reported by other authors for LEO and GSE alone or in combination with other preservatives (Xu et al. 2007a; Viuda-Martos et al. 2008; Perdonés et al. 2012; Kanmani and Rhim 2014; Teixeira et al. 2013). Likewise, these concentrations are higher than the minimum inhibitory one for LEO and GSE (Xu et al. 2007a). The maximum concentration used was limited considering that the essential oil added does not notably change the sensory characteristics of the film, especially its color and odor.

Glycerol was added as plasticizer in all formulations at 25 % w/w with respect to the polymers, according to previous studies (Bof et al. 2015). Likewise, the plasticized 75:25 CS/CH blend was used as control film.

Dispersions were homogenized at 13,500 rpm for 1 min and at 20,500 rpm for 45 s, under vacuum to avoid bubble formation, by using a venture vacuum pump connected to a rotor stator homogenizer (Ultraturrax T25, Janke and Kunkel, Germany). Finally, five film formulations were obtained and named GSE1 %, GSE3 %, LEO1 %, LEO3 %, and Control. Table 1 shows the mass fraction of the different film components with respect to the total film solids for each formulation, together with the equivalent total amount of solids poured into each plate.

**Table 1** Mass fraction ( $X$ ) of different compounds ( $S$  starch,  $CH$  chitosan,  $Gly$  glycerol, GSE solids and LEO) in the dry solids of the different film samples and equivalent solid mass poured per plate (Sm/p: g)

Sample	$X_S$	$X_{CH}$	$X_{GLY}$	$X_{GSE}$	$X_{LEO}$	Sm/p (g)
Control	0.662	0.138	0.20	–	–	1.886
GSE1 %	0.651	0.136	0.20	0.0163	–	1.897
GSE3 %	0.631	0.131	0.19	0.0473	–	1.920
LEO1 %	0.542	0.113	0.16	–	0.181	2.280
LEO3 %	0.398	0.083	0.12	–	0.398	3.044

### Rheological Behavior of Film-Forming Dispersion

The rheological behavior of FFDs was analyzed using a rotational rheometer (Paar Physica Rheolab MC1, Graz, Austria) with the geometry of coaxial cylinders at 25 °C. Samples were left to rest for 5 min before testing. Two scans (ramp up and ramp down) were carried out from 0 to 500 s<sup>-1</sup> and from 500 to 0 s<sup>-1</sup>. The flow curves, shear stress as a function of shear rate, were obtained. The Ostwald de Waele (Eq. 1) model was used to fit the experimental data.

$$\sigma = K \times \gamma^n \quad (1)$$

where  $K$  is the consistency index and  $n$  is the flow behavior index. FFDs were analyzed at least in duplicate.

### Film Preparation, Conditioning, and Characterization

Films were obtained by casting method. FFD (42 g) was spread onto Teflon plates of 15 cm in diameter and were left for approximately 48 h at 20 °C and 45 % RH on a leveled surface until drying. Films were conditioned before tests for 1 week in a desiccator at 25 °C and 53 % RH, by using Mg(NO<sub>3</sub>)<sub>2</sub>·6H<sub>2</sub>O oversaturated solutions (Panreac Química, SA, Castellar del Vallès, Barcelona).

The moisture of the conditioned films was determined by drying the samples in a natural convection oven at 60 °C for 24 h and then for another 24 h at 60 °C in a vacuum oven. Determinations were carried out at least in triplicate. Film thickness was measured with a Palmer digital micrometer (Palmer–Comecta, Spain) to the nearest 1 μm at six random positions.

### Effective Essential Oil Content of Active Blend Films

Since LEO is rich in volatile compounds that could be lost during film preparation, the effective essential oil content in the dry-blend film was quantified. The active compounds of the film samples (about 0.10 g) were extracted with diethyl ether (10 ml) while the system was maintained under stirring for 24 h before testing.

The essential oil content of the films was determined in a gas chromatograph (Fisons GC 8060, Italy) equipped with a flame ionization detector (GC-FID) and a DB-5 capillary column of 30 m × 0.32 mm I.D. and 0.25 μm stationary phase film thickness (J&W Scientific Agilent, Palo Alto, USA). Helium was used as the carrier gas at a flow rate of 1 mL min<sup>-1</sup>. In all cases, 2 μl of film extract were injected. The oven was programmed as follows: initial temperature 50 °C, ramped at 5 °C/min to 130 °C, held for 5 min at 130 °C, and then ramped at 10 °C/min to 200 °C. The injector and detector temperatures were set at 250 °C. The calibration curve was obtained by using (R)-(+)-Limonene (Merck, USA) as standard at different concentrations. The total amount of essential oil retained in the films was estimated by taking into account the mass fraction of limonene in the LEO, which was also determined by the same method, using a diethyl ether LEO solution of known concentration.

### Film Optical Properties

The surface reflectance spectra of the films were determined between 400 and 700 nm using a spectrophotometer CM-3600d (Minolta Co., Tokyo, Japan) on a white and black background. The Kubelka–Munk theory for multiple scattering was applied to the reflection spectra to determine the films' transparency. Internal transmittance was calculated according to the following Eqs. (2) to (4):

$$Ti = \sqrt{(a-R_0)^2 - b^2} \quad (2)$$

$$a = \frac{1}{2} \left( R + \frac{R_0 - R + R_g}{R_0 R_g} \right) \quad (3)$$

$$b = \sqrt{a^2 - 1} \quad (4)$$

where  $R_0$  is the reflectance of the sample on an ideal black background and  $R$  is the reflectance of the film backed by a known reflectance,  $R_g$ . Measurements were taken at least in triplicate. CIEL\*a\*b\* color parameters were obtained from the infinite reflectance ( $R_\infty$ ) data calculated, by considering 10° observer and D65 illuminant reference, according to Ortega-Toro et al. (2015).

The surface film gloss was measured using Multigloss 268 equipment (Konica Minolta, Germany), and the results were expressed at 60° of light incidence, according to the ASTM standard D523 method (ASTM 1999).

### Water Solubility

Film solubility was determined by keeping a 2-cm<sup>2</sup> film sample in bidistilled water in a film/water ratio of 1:100 w/w, for 72 h at 25 °C. Three replicates were considered for each

formulation. After 72 h, the film samples were transferred to a convection oven (J.P. Selecta, S.A., Barcelona, Spain) for 24 h at 60 °C to remove free water and afterward transferred to a vacuum oven for 24 h at 60 °C. Finally, the solubility was calculated as the difference of the dry weight at the beginning and end of the process divided by the initial dry weight and expressed as a percentage.

### Tensile Properties

The tensile behavior of films was analyzed by using a universal test machine (TA.XT plus model, Stable Micro Systems, Haslemere, England) with a tension grip system A/TG. Probes of 2.5 cm wide and 10 cm long were cut from the conditioned films and mounted in the film extension grips of the machine and stretched until breaking at 50 mm/min speed test. Tensile strength (TS), elastic modulus (EM), and elongation at break (EB) were calculated according to ASTM standard method D882 (ASTM 2001) from stress–strain curves, which were obtained from force–distance data. The test was performed at 25 °C and 53 % RH. At least eight probes were tested from each formulation.

### Barrier Properties

Water vapor permeability of the films was determined by using the ASTM E96-95 (ASTM 1995) gravimetric method, taking into account the modification of the previous standard proposed by McHugh et al. (1993). Films were placed in Payne permeation cells (3.5 cm in diameter and 9.62 cm<sup>2</sup> of area, Elcometer SPRL, Hermelle/s Argenteau, Belgium), which were previously filled with distilled water to ensure a 100 % relative humidity on one side of the film. Then, cups were placed in cabinets with oversaturated solutions of Mg(NO<sub>3</sub>)<sub>2</sub>·6H<sub>2</sub>O (Panreac Química, SA, Castellar del Vallès, Barcelona) in order to obtain 53 % RH at 25 °C. Cabinets were fitted with a variable-speed fan to provide a strong driving force across the film for water vapor diffusion. After the steady-state condition was reached, the cells were weighed (0.0001 g) at a 1-h interval for 8 h. The water vapor transmission rate (WVTR) was calculated from the slope of the weight loss versus time data-fitted straight line.

The vapor pressure on the films' inner surface ( $p_2$ ) was obtained with Eq. (5), proposed by McHugh et al. (1993), to correct the effect of concentration gradients established in the stagnant air gap inside the cup:

$$\text{WVTR} = \frac{\text{PDL}_n \left[ \frac{P - p_2}{P - p_1} \right]}{RT \Delta z} \quad (5)$$

where  $P$  is the total pressure,  $D$  is diffusivity of water through air at 25 °C,  $R$  is the gas law constant,  $T$  is the absolute

temperature,  $\Delta z$  is the mean stagnant air gap height,  $p_1$  is the water vapor pressure on the solution surface, and  $p_2$  is the corrected water vapor pressure on the film's inner surface. Water vapor permeance was calculated according to Eq. (6):

$$\text{Permeance} = \frac{\text{WVTR}}{P_2 - p_3} \quad (6)$$

where  $p_3$  is the pressure on the film's outer surface in the cabinet. Finally, the water vapor permeability is obtained as the permeance multiplied by the thickness of the sample. The test was carried out in quadruplicate.

Likewise, the oxygen permeation of the films was determined in an OX-TRAN Model 2/21 ML Mocon (Lippke, Neuwied, Germany) at 25 °C and 53 % RH. The test was conducted at 25 °C and 53 % RH and the exposure area of the samples was 50 cm<sup>2</sup>. The samples were conditioned in the cells for 6 h, and then the transmission values were taken every 20 min until the equilibrium was reached. The thickness of the films was considered to obtain the oxygen permeability, and the results were expressed in cm<sup>3</sup> s<sup>-1</sup> m<sup>-1</sup> Pa<sup>-1</sup>.

### Film Thermal Properties

#### Thermogravimetric Analysis

The thermal analysis of the films was performed in a thermobalance TGA 1 Stare System analyzer (Mettler-Toledo, Inc., Switzerland). The conditioned samples were heated from 25 to 600 °C at a rate of 10 °C/min, using nitrogen flow (250 mL/min). The equipment registered both the weight loss (TG) and the derivative (DTG); thermal degradation temperature ( $T_{\text{peak}}$ ) was obtained at the maximum of the DTG curves. Two replicates per formulation were analyzed.

#### Differential Scanning Calorimetry

Differential scanning calorimetry (DSC) analyses were performed using a DSC 1 Star<sup>c</sup> System (Mettler-Toledo, Inc., Switzerland). Film samples (about 10 mg) were put into aluminum pans and sealed; an empty pan was used as reference. The equipment registered the heat flow as a function of temperature; two scans were performed. Pans were heated from 0 to 200 °C at a rate of 10 °C/min, where the bonded water was eliminated from the films, and the previous thermal history of the material was deleted. Then, in a second step, the samples were cooled to 0 °C and finally heated to 200 °C at the same heating rate. The observed glass transition was identified as the midpoint temperature. At least two samples of each formulation were analyzed.



## Scanning Electron Microscopy

The microstructural analysis was carried out by using a scanning electron microscope (JEOL JSM-6300, Japan). Prior to SEM analysis, the samples were put in desiccators with  $P_2O_5$  to remove water which could interfere with the observations. The films were frozen with liquid nitrogen and then cryofractured for cross-section observations. The small pieces were mounted on copper stubs and then coated with gold. The accelerating voltage was fixed at 10 kV for all observations.

## Fourier-Transformed Infrared Spectroscopy

Fourier-transformed infrared (FTIR) spectra of the films were obtained with an IR spectrophotometer (Bruker, Karlsruhe, Germany) equipped with a platinum ATR optical cell and an RT-D1a TGS detector, by using total attenuated reflection mode (ATR-FTIR). Spectra were recorded between 4000 and 400  $cm^{-1}$  by accumulation of 64 scans at 4  $cm^{-1}$  resolution. Data were treated using OPUS software (Bruker, Karlsruhe, Germany). Initial absorbance spectra were smoothed using a nine-point Savitsky-Golay algorithm, and elastic baseline correction (200 points) was applied. Then, these were centered and normalized using the abovementioned software.

## Antimicrobial and Antioxidant Activity

The antimicrobial capacity of the films was determined according to the method described by Tepe et al. (2005), with some modifications related with the cell concentration and the film disk diameter used. The microorganisms chosen for the test were some molds (*Alternaria alternata*, *Rhizopus stolonifer*, *Penicillium expansum*) and one Gram+ and one Gram– culture bacteria (*Listeria innocua* and *Escherichia coli*). The chosen molds are commonly associated to fruit deterioration while the bacteria are related to common foodborne diseases. All microorganisms were purchased from Colección Española de Cultivos Tipo (Burjassot, Valencia, Spain) and kept frozen in potato dextrose broth (PDB) for molds and tryptic soy broth (TSB) for bacteria, both supplemented with 30 % glycerol as cryoprotector agent.

The molds' spores were counted in a Thoma counting chamber and diluted in PDB to reach a concentration of  $10^5$  spores/ml. On the other hand, culture bacteria were diluted in TSB to  $10^5$  CFU/ml. The diluted spore suspensions of molds and bacteria were inoculated (100  $\mu$ l) on Petri dishes containing potato dextrose agar (PDA) and tryptic soy agar (TSA), respectively, and extended by using a Digrafsky spatula.

Film samples were cut in 2-cm diameter circles and placed on the inoculated dishes. At the same time, sterile paper disks

with the same diameter were impregnated with pure GSE and pure LEO, at the same concentration as that present in the less concentrated films, and placed on the inoculated dishes. All plates were incubated for 48 h at 25 °C for molds and 24 h at 37 °C for bacteria. After this time, inhibition zone diameter was measured. Tests were performed at least in triplicate.

The antioxidant activity of the active compounds and films was evaluated by means of the Trolox equivalent antioxidant capacity (TEAC), using a modification of the method described by Re et al. (1999). The purpose of the method is to compare the antioxidant activity of the analyzed substance with the activity of an antioxidant standard, Trolox (6-hydroxy-2,5,7,8-tetramethylchroman-2-carboxylic acid), a vitamin E analog. According to this method, the ABTS (2,2-azino-bis[3-ethylbenzothiazoline-6-sulphonic acid]) reactive was dissolved in water to obtain a 7 mM solution, and then allowed to react with a 2.45 mM potassium persulfate solution for 16 h in the dark. The ABTS radical cation (ABTS<sup>•+</sup>) obtained, a blue chromophore, was diluted with a water/methanol (2:8) solution until initial absorbance of 0.70(±0.02) at 734 nm. The measurements were taken with a Beckman Coulter DU 730 spectrophotometer, using a water/methanol (2:8) solution as blank. The test solutions were prepared by dissolving the films (180 mg) in 10 ml of water/methanol (2:8) blend to favor the extraction of antioxidant components (Jiménez et al. 2013a). Solutions of LEO and GSE at different concentrations were prepared in the same water/methanol solvent and analyzed for their absorbance reduction capacity. The percentage of absorbance reduction at 6 min was registered when 10  $\mu$ l of the test solution was added to 990  $\mu$ l of the ABTS radical dilution. For calibration purposes, Trolox standards of different concentrations (0 to 200 mg/l) were prepared and the same procedure was followed. The results were obtained from percent absorbance vs. concentration curves and expressed as the concentration needed to produce the same absorbance reduction as 1 mM solution of Trolox (TEAC). All tests were performed in triplicate.

## Statistical Analysis

All results were statistically analyzed by using the software Statgraphics Plus for Windows 5.1 (Manugistics Corp., Rockville, MD) through analysis of variance (ANOVA). Means were compared with Fisher's least significant difference (LSD) at 95 % confidence level. The relationship between physicochemical, barrier, mechanical, and optical properties was studied using explorative principal component analysis (PCA) with InfoStat software (version 2008; InfoStat Group, National University of Cordoba, Argentina).

## Results and Discussion

### Rheological Behavior of Film-Forming Dispersion and Film Microstructure

All FFDs presented a shear-thinning behavior ( $n < 1$ ), which was satisfactorily adjusted by the Ostwald de Waele model (Table 2) and no time dependence was observed since up and down curves coincided. The addition of natural active agents affected the rheological behavior of FFDs. GSE incorporation hardly affected rheological behavior due to the low solid content of the extract and its solubility in the aqueous FFD. Nevertheless, at the highest ratio, a significant ( $p < 0.05$ ) increase in the flow index  $n$  occurred, which can be due to the influence of the solid extract on the solvent goodness for polymers, thus partially inhibiting the chain unfolding in the aqueous media. FFDs containing LEO were more viscous and exhibited higher shear-thinning character than did those containing GSE, according to the presence of an oil-dispersed phase.

The rheological behavior of filmogenic formulations reflect differences in the microstructure of the FFDs introduced by active compounds in the aqueous media: GSE solids slightly affect the compound arrangement whereas LEO introduced a new dispersed phase (oil droplets) due to its non-solubility in the aqueous medium, all of this affecting the final film microstructure.

SEM micrographs of the control films show a homogeneous phase that can be attributed to the compatibility and miscibility of both polymers (Fig. 1a). The GSE1 % and GSE3 % film micrographs exhibit the same continuous and smooth aspect than do the control ones (Fig. 1b, c), in agreement with the compound compatibility, as deduced from the rheological behavior of the FFDs. However, in LEO1 % and LEO3 % samples, the presence of oil droplets embedded in the polymers' matrix can be clearly observed (Fig. 1d, e). LEO3 % samples present bigger droplets in line with the higher concentration of dispersed phase and the subsequent promotion of droplet flocculation during the film drying step. Oil droplets introduced discontinuities in the polymer network which could affect the mechanical behavior and barrier properties of the films (Jiménez et al. 2013b).

**Table 2** Ostwald de Waale rheological parameters and apparent viscosity at  $100 \text{ s}^{-1}$  of the film-forming dispersions

Sample	Number	$k$ ( $\text{Pa s}^n$ )	$\eta_{\text{ap}}$ ( $\text{mPa s}$ )
Control	0.93 (0.02)b	0.048 (0.006)c	34.0 (1)c, d
GSE1 %	0.961 (0.015)a	0.047 (0.004)c	39.0 (0.3)b
GSE3 %	0.966 (0.009)a	0.039 (0.002)c	33.0 (0.6)d
LEO1 %	0.880 (0.018)c	0.061 (0.006)b	35.0 (0.8)c
LEO3 %	0.8620 (0.0009)c	0.0780 (0.0005)a	41.0 (0.7)a

Standard deviations are shown between parentheses. Different lowercase letters indicate significant differences among formulations ( $p < 0.05$ )

### Film Thickness, Water Solubility, and Lemon Essential Oil Retention

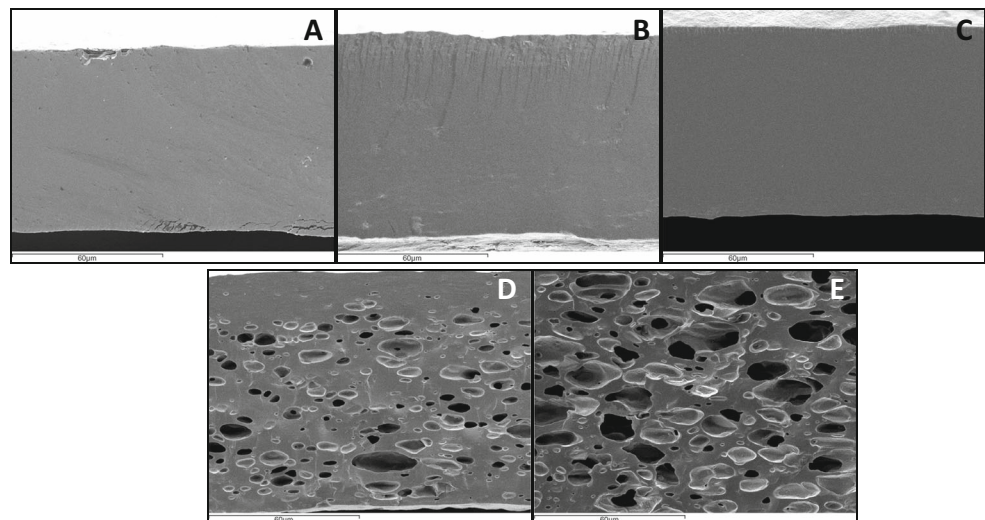
The blend films with LEO or GSE were visually homogeneous since no phase separation between the components was visually detected; likewise, they could be easily separated from the plates. Films thickness was different because of the differences in the total solid content of the formulations and so the different solid mass poured per plate (Table 1). GSE addition did not notably affect film thickness due to the low solid content of the GSE extract while LEO led to thicker ones in line with the greater amount of the poured solids in the plate (Table 1). Meanwhile, solubility at  $25 \text{ }^\circ\text{C}$  (Table 3) was affected by essential oil content: the higher the oil concentration, the lower the film solubility due to the increase of the hydrophobic character of the matrix when lipid was added. The incorporation of GSE did not significantly affect film solubility probably due to its low mass fraction in the films and its more hydrophilic nature. The equilibrium moisture content of the films followed a similar trend to water solubility. Ghasemlou et al. (2013) found similar effects when essential oils were added into biopolymer matrices, which can be explained by the decrease in the global ratio of active points for water interactions when a hydrophobic phase is present in the film matrix.

Considering the hydrophilic nature of GSE, its good incorporation in the matrix can be expected. Meanwhile LEO composition includes non-water-soluble volatile compounds, which can evaporate during the film drying step, together with water at the film surface (steam distillation). Thus, film lipid extracts were analyzed by gas chromatography to quantify the final amount of LEO components present in the samples. The limonene is the main component of the lemon essential oil, varying its quantity with the essential oil source and the extraction procedure, as was previously mentioned. The chromatographic analysis allowed calculating the limonene content in the used lemon essential oil as well as that incorporated into the film formulations. Limonene content in the LEO was 66 %. From the determined amount of limonene in the films, its retention percentage in dried films was estimated, taking into account the nominally incorporate essential oil. The estimated losses of limonene during the film formation process were  $69 \pm 3 \%$ , regardless of the initial content in the FFD. From this data, and assuming that similar losses occurred for the other LEO compounds, the remaining content of the essential oil in the dried films was 0.061 and 0.117 g/g solids for LEO1 % and LEO3 % samples, respectively.

### Film Optical Properties

The optical properties (gloss  $60^\circ$  and internal transmittance at 450 nm) and color parameters of the films are presented in Table 4. The  $h_{\text{ab}}^*$  and  $C_{\text{ab}}^*$  parameters indicate that all the

**Fig. 1** SEM micrographs of chitosan–corn starch-blend films: **a** control, **b** GSE 1 %, **c** GSE 3 %, **d** LEO 1 %, and **e** LEO 3 %



films had a yellowish color, which was in agreement with visual observations. Films with 3 % LEO and 3 % GSE presented higher color differences ( $\Delta E^*$ ) with respect to the control film than those containing 1 % of both components. In general, the addition of active compounds increased  $C_{ab}^*$ , 18.7 and 51.4 % for 3 %GSE and 3 %LEO, respectively. While considering the lightness parameter  $L^*$ , 3 %GSE or 3 %LEO films showed lower values than did the control films (6.2 and 3.6 % decrease).

Likewise, the gloss values were higher for films with LEO; meanwhile, films with GSE exhibited significantly lower values, as compared with the control. The increase in gloss promoted by LEO could be attributed to the fact that free lipids acted as fillers of the micropores at the film surface, thus reducing the surface roughness and enhancing the gloss (Ortega-Toro et al. 2014; Villalobos et al. 2005).

All the films were highly transparent according to the internal transmittance values, although it was reduced by the incorporation of active agents, mainly at higher concentration and especially for films containing LEO (Table 4). The presence of a dispersed phase in the films which promotes light scattering is responsible for this effect (Jiménez et al. 2012).

**Table 3** Moisture content, water solubility (dissolved solid percentage regarding the total solids), and thickness of the chitosan–corn starch blend films

Sample	Moisture (g/100 g)	Solubility (%)	Thickness ( $\mu\text{m}$ )
Control	10.5 (0.8) <sup>b</sup>	25.71 (0.05) <sup>a</sup>	80 (4) <sup>c</sup>
GSE1 %	10.4 (0.4) <sup>b</sup>	24.7 (0.3) <sup>a</sup>	81 (4) <sup>c</sup>
GSE3 %	11.6 (0.5) <sup>a</sup>	26.1 (0.7) <sup>a</sup>	79 (5) <sup>c</sup>
LEO1 %	8.97 (0.14) <sup>c</sup>	23.7 (0.5) <sup>a</sup>	113 (7) <sup>b</sup>
LEO3 %	8.67 (0.01) <sup>c</sup>	20 (3) <sup>b</sup>	162 (10) <sup>a</sup>

Standard deviations are shown between parentheses. Different lowercase letters indicate significant differences among formulations ( $p < 0.05$ )

Therefore, the incorporation of GSE or LEO provoked changes in the optical properties of the CS–CH films, depending on their concentration. Films became slightly darker and yellowish and less transparent. GSE reduced the film gloss, whereas LEO led to glossier films; all this enhanced when the active concentration increased in the films.

### Tensile and Barrier Properties

Table 5 presents the tensile parameters of chitosan–corn starch blend films: tensile strength (TS, MPa), elongation at break (EB, %), and elastic modulus (EM, MPa), which are closely related with the film microstructure. As it is well known, TS represents the resistance to break; meanwhile, EB describes the stretching capacity and EM represents the stiffness of the films. The tensile behavior of the films was strongly affected by the incorporation of GSE and LEO, both components leading to films being less stiff and resistant to break (lower TS values) but more stretchable (higher EB values) than the control ones. This decrease in stiffness and increase in extensibility could be attributed to the weakening of the polymer network forces in line with the presence of other compounds (solubilized or dispersed), which interrupt the chain entanglements. LEO produced more marked effects due to its higher concentration in the matrix and the lack of polymer miscibility, which introduced a great number of discontinuities in the matrix as can be observed in the SEM micrographs (Fig. 1). Nevertheless, the induced increase in the film stretchability caused by essential oil indicates that it not only provoked matrix discontinuities but also interacted with the polymer chains, enhancing their capability to slip during the tensile test, thus promoting film extensibility, as reported by other authors (Sánchez-González et al. 2010; Kavosi et al. 2013; Tongnuanchan et al. 2012; Bonilla et al. 2011). GSE addition also enhanced film stretchability, although its effect on the TS and EM was minor. These results also suggest the

**Table 4** Color parameters, gloss, and transparency of the chitosan–corn starch blend films

Sample	L*	C <sub>ab</sub> *	h <sub>ab</sub> *	ΔE	Gloss (60°)	Ti (450 nm)
Control	78.8 (0.7)ab	17.3 (0.7)c	88.8 (0.5)a	–	26.2 (1.3)b	81.3 (0.6)a
GSE1 %	77.3 (0.9)bc	18.1 (0.7)c	87.4 (0.7)c	1.8 (1.3)c	15.5 (1.5)c	80.9 (1.4)a
GSE3 %	73.9 (0.3)d	20.5 (0.2)b	84.76 (0.03)d	6.0 (0.2)b	12.0 (1.2)c	78.3 (0.2)b
LEO1 %	79.4 (1.2)a	17.7 (2)c	88.5 (0.4)ab	2.4 (0.9)c	37 (4)a	80.8 (0.6)a
LEO3 %	76.0 (0.3)c	26.2 (0.2)a	87.80 (0.09)bc	9.3 (0.3)a	30 (4)b	72.94 (0.03)c

Standard deviations are shown between parentheses. Different lowercase letters indicate significant differences among formulations ( $p < 0.05$ )

development of interactions with polymer chains without producing discontinuities in the matrix due to the greater compatibility among GSE components and polymer molecules.

Table 5 also shows the water vapor and oxygen barrier properties of the films, where no notable effect of the incorporated active compounds can be observed.

It was expected that the incorporation of an oil phase in the films reduces the water molecule permeation because of its hydrophobic nature and the tortuosity increase in the matrix pathway, all this enhancing the water vapor resistance through the film (Sánchez-González et al. 2010). However, this effect was not notably observed for LEO films. Kanmani and Rhim (2014) working on agar-based films also reported that the water vapor barrier property was not affected by the incorporation of GSE in similar concentrations than those used in the present study. These authors also remark that some controversial results about the effect of the essential oil addition on the water vapor permeability (WVP) of films have been reported (Hong et al. 2009; Song et al. 2012; Lim et al. 2010; Jang et al. 2011).

Likewise, oxygen permeability was not affected by GSE incorporation, maintaining the active films' similar efficiency as oxygen barriers to those based on polysaccharides. In the case of films containing LEO, oxygen permeability could not be measured because of equipment restrictions, since volatile compounds affect the sensitivity of the equipment sensor.

**Table 5** Tensile and barrier properties of the chitosan–corn starch blend films

Sample	EM (MPa)	TS (MPa)	EB (%)	WVP (g mm kPa <sup>-1</sup> h <sup>-1</sup> m <sup>-2</sup> )	OP 10 <sup>-14</sup> (cm <sup>3</sup> m <sup>-1</sup> s <sup>-1</sup> Pa <sup>-1</sup> )
Control	151 (20)a	18.3 (1.9)a	57 (3)d	7.5 (0.4)a	7.7 (0.2)a
GSE1 %	120 (8)b	14.6 (1.1)b	58.3 (1.3)cd	7.8 (0.2)a	8.2 (0.7)a
GSE3 %	63 (12)d	14.4 (1.9)b	67 (4)a	7.5 (0.4)a	8.47 (0.11)a
LEO1%	84 (6)c	11.8 (0.8)c	62 (2)bc	7.5 (0.4)a	–
LEO3%	30 (12)d	6.7 (1.4)d	66 (6)ab	7.4 (0.3)a	–

Standard deviations are shown between parentheses. Different lowercase letters indicate significant differences among formulations ( $p < 0.05$ )

EM elastic modulus, TS tensile strength, EB elongation at break, WVP water vapor permeability, OP oxygen permeability

## Thermal Behavior

Figure 2 shows the weight loss versus temperature curves for films obtained by TGA(A), together with the derivative (DTGA) curve (B). All formulations show an initial peak up to about 100 °C, which can be attributed to the loss of bonded water in the film (Luo et al. 2012). Afterward, a second weight loss step can be observed in LEO films, which can be attributed to the volatile release, and finally, at around 275 °C, degradation of both polymers occurs (Martínez-Camacho et al. 2010). It can be noticed that the LEO films had higher weight loss than did the GSE and control ones due to the loss of essential oil.

Table 6 shows thermal degradation temperature at the maximum degradation rate ( $T_{peak}$ ), weight loss obtained by thermogravimetric analysis (TGA), and glass transition temperature ( $T_g$ ) registered in the DSC analysis. Tg was recorded in the second heating scan of DSC analysis to avoid the effect of bonded water in the film in the first scan. Incorporation of GSE or LEO did not significantly affect the glass transition temperature of the films, which can be attributed to the starch phase and values appearing in the range that was previously reported for the plasticized corn starch film (Ortega-Toro et al. 2015). No thermal response of glass transition temperature was observed for the chitosan materials.



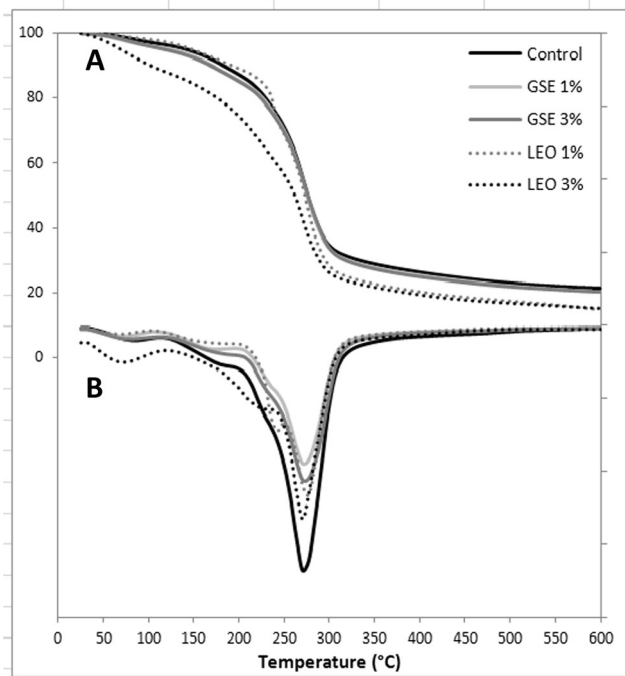


**Fig. 2** Thermogravimetric (TG, **a**) and its first derivative (DTG, **b**) curves of chitosan–corn starch blend films

### Principal Component Analysis

A PCA was carried out, taking the main film properties into account, for the purposes of comparing the different formulations. Figure 3 presents the PCA of the first two principal components (PC1 and PC2) of composite films containing GSE or LEO as active compounds at the concentrations tested. PC1 and PC2 explained 90.8 % of the variance (63.6 % PC1). In terms of PC1, the control film and those containing GSE (1 and 3 %) are very close, whereas films containing LEO (especially LEO3%) were more differentiated (Fig. 3). PC2, which explain a much lower percentage of variance, only notably separate films with different ratios of GSE, probably due to the impact of the GSE concentration on some film properties such as tensile parameters and  $T_g$ , as previously commented. Therefore, from the PCA analysis, the main

**Table 6** Main degradation temperature ( $T_{peak}$ ) of polymer, weight residue of thermal degradation at 500 °C, and starch phase glass transition temperature ( $T_g$ ) of the chitosan–corn starch blend films

Sample	$T_{peak}$ (°C)	% weight residue	$T_g$ (°C)
Control	272.3 (0.4)b	23.4 (0.6)a	110.2 (6)a,b
GSE 1 %	273.3 (1.4)b	22.7 (0.7)a	115.2 (1.6)a
GSE 3 %	273.4 (0.4)b	22.4 (0.9)a	104.7 (1.2)b
LEO 1 %	275.2 (0.3)a	17.4 (0.2)b	113.3(1.6)a
LEO 3 %	270.6 (0.9)c	16.3 (1.9)b	113.4 (0.2)a

Standard deviations are shown between parentheses. Different lowercase letters indicate significant differences among formulations ( $p < 0.05$ )

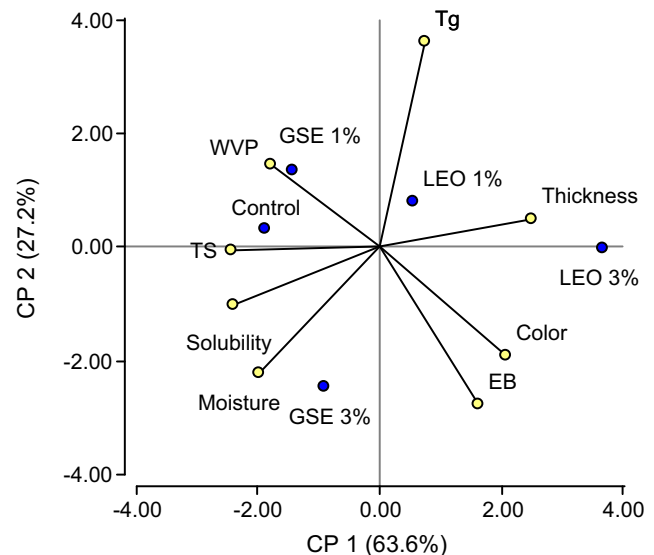


**Fig. 3** Principal component analysis of the first two principal components (PC1 and PC2) of chitosan–corn starch blend films containing GSE or LEO as active compounds at different concentrations (1 and 3 %). WVP water vapor permeability, TS tensile strength, EB elongation at break and  $T_g$  glass transition temperature

difference among the formulations was introduced by LEO, in agreement with the lack of miscibility of its components with the polymer chains and the presence of a dispersed phase into the polymer matrix.

### Fourier-Transformed Infrared Spectroscopy

Figure 4a, b show the FTIR spectra obtained for the pure components and blend films, respectively, in order to compare the band positions and to detect possible displacements. The broad band located at  $3290\text{ cm}^{-1}$ , observed for pure corn starch, chitosan, and GSE, corresponds with vibration modes of  $-\text{OH}$  groups from the absorbed water and the polymer itself (Garcia et al. 2009). The peaks at  $2920$  and  $2871\text{ cm}^{-1}$  are related with  $\text{CH}_2$  y  $\text{CH}_3$  groups (Zhang et al. 2012).

From the pure chitosan spectrum, two characteristic bands can be noticed: the amide I band, at  $1643\text{ cm}^{-1}$ , corresponding to carbonyl stretching, and the amide II band, corresponding to  $\text{NH}_2$  bending at  $1575\text{ cm}^{-1}$  (Duarte et al. 2002). The peaks exhibited at  $1151$  and  $1064\text{ cm}^{-1}$  in the chitosan spectra correspond to an asymmetric stretching of the  $\text{C}-\text{O}-\text{C}$  bridge and skeletal vibrations involving  $\text{C}-\text{O}$  stretching, respectively, being both typical of chitosan (Rivero et al., 2010). The sharp peaks at  $1020\text{ cm}^{-1}$  are related with  $\text{C}-\text{O}$  stretching vibrations (Zhang et al. 2012; Jiménez et al. 2014).

In the LEO spectra, there is a main peak at  $890\text{ cm}^{-1}$  related with  $\text{C}-\text{H}$  stretching, which is characteristic of aromatic compounds (Sánchez Aldana et al. 2014). Likewise, the stronger asymmetric band at around  $3100\text{--}2850\text{ cm}^{-1}$ , underlying the presence of aliphatic and unsaturated hydrocarbons related to terpenoid components, presents in LEO. The GSE spectra

**Fig. 4** FTIR spectra of the different components (a) and chitosan–corn starch blend films (b)

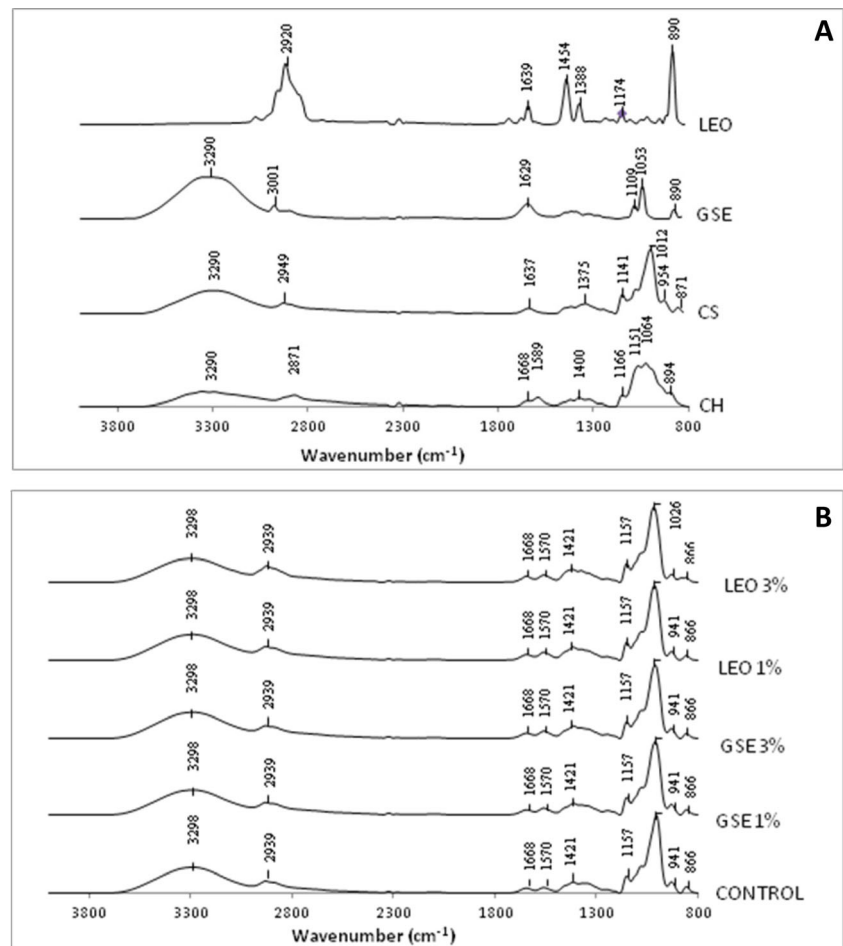


exhibit a wide absorption band at 3600–3100  $\text{cm}^{-1}$ , related to typical OH vibrations of aromatic/phenolic compounds (Boumailet al. 2013), revealing the hydrophilic character of this active compound. Besides, the peak at 890  $\text{cm}^{-1}$  previously described is also observed in the GSE spectra. On the other hand, the films' spectra were all similar due to their similar composition. The FTIR spectra of the blend films exhibited the typical signals of both starch and chitosan. The amplitude increase of 3300  $\text{cm}^{-1}$  signal in the blend films is indicative of the development of hydrogen bonding interactions in the blend films, which is the predominant interaction mechanism between hydrophilic polymers. The spectra of composite films presented small modifications in the position of some bands within the range of 1500–1700  $\text{cm}^{-1}$  that are related to amino and carbonyl groups, thus indicating effective interactions between starch and chitosan chains.

Likewise, in CH-based films, the appearance of a shoulder at 1460–1457  $\text{cm}^{-1}$  was observed and attributed to the stretching of the  $\text{CH}_2$  group (Wilhelm et al. 2003; Bof et al. 2015). This signal indicates that the plasticizer added was bonded to the polymeric chains.

Furthermore, there is no evidence of chemical reactions between the components because of the lack of new covalent bonds in the spectra (Jiménez et al. 2014).

#### Antimicrobial and Antioxidant Activities of the Films

The results of the antimicrobial test are shown in Table 7. The pure LEO exhibited antimicrobial activity only in the case of Gram+ bacteria. A similar trend was observed for films containing LEO and, as can be expected, its activity increases with the compound concentration. In the case of GSE, it was effective against Gram + and Gram- only when it was applied directly in the paper disks (pure GSE). Similar results of GSE antimicrobial activity against *E. coli* and *L. monocytogenes* were reported by Kanmani and Rhim (2014). The Gram-pathogens were less susceptible than the Gram+ ones, probably because of the fact that the first ones have an additional membrane on their cells, which could hinder the diffusion of antimicrobial compounds. However, the GSE1 % and GSE3 % films did not show antimicrobial activity, which can be attributed to the low active concentration diffused to

**Table 7** Antimicrobial activity of the chitosan–corn starch blend films and pure GSE and LEO against several molds and bacteria using disk diffusion method

	Control	GSE1 %	GSE3 %	Pure GSE	LEO1 %	LEO3 %	Pure LEO
<i>Listeria innocua</i>	NA (-)	NA (-)	NA (-)	30.76 (2.53)bcA (-)	29.25 (3.08)c (-)	34.42 (4.11)b (-)	39.43 (3.09)A (-)
<i>Escherichia coli</i>	NA (-)	NA (-)	NA (-)	22.13 (0.21)b (-)	NA (-)	NA (-)	NA (-)
<i>Alternaria alternata</i>	NA (+)	NA (+)	NA (+)	NA (+)	NA (-)	NA (-)	NA (+)
<i>Rhizopus stolonifer</i>	NA (-) <sup>a</sup>	NA (-) <sup>a</sup>	NA (-) <sup>a</sup>	NA (-) <sup>a</sup>	NA (-) <sup>a</sup>	NA (-) <sup>a</sup>	NA (-) <sup>a</sup>
<i>Penicillium expansum</i>	NA (-) <sup>a</sup>	NA (-) <sup>a</sup>	NA (-) <sup>a</sup>	NA (-) <sup>a</sup>	NA (-)	NA (-)	NA (-)

Standard deviations are shown between parentheses. Different lowercase letters within the same line indicate significant differences among formulations ( $p < 0.05$ ). Different uppercase letters within the same row indicate significant differences among formulations ( $p < 0.05$ ). (+) and (-) indicate growth or non-growth, respectively, below the film disk

NA non-active

<sup>a</sup> Microorganism growth over the film disk

the culture media, which did not reach the minimal inhibitory concentration (MIC) for the tested microorganisms. Thus, release kinetics of active compounds must be assessed to understand antimicrobial activity. Pure components did not show antifungal activity against the fungi tested at the used concentrations.

Antioxidant activity of pure GSE and LEO was quantified in terms of Trolox equivalent antioxidant capacity (TEAC) values and was 143 and 157 g/l, respectively, for GSE and LEO, respectively, which supposes an antioxidant activity much lower than Trolox (the same absorbance reduction was produced by 250.29 mg/l of Trolox). However, the film extracts containing both GSE and LEO did not produce significant reduction of the absorbance values in the test, which can be attributed to the insufficient amount of active compounds. Even assuming their total extraction from the films, the concentration levels in the extract should be much lower than the TEAC values (2.2 g/l in the best of the cases: LEO 3 %).

## Conclusions

Chitosan–starch-based composite films incorporating LEO and GSE as potential active components exhibited a yellowish color, with this characteristic more marked in the case of LEO films at the highest concentration. SEM micrographs evidenced a homogenous incorporation of GSE to film matrix, while oil droplets were dispersed in the LEO film matrix. Tensile properties were affected by the incorporation of active compounds and their concentration, the films being less stiff and resistant but more stretchable than control films were, although they did not modify the oxygen and water vapor barrier properties of the films. Therefore, biodegradable chitosan–starch blend films with the incorporation

of LEO and GSE, having good functional properties and antibacterial activity, is promising to be used as a biodegradable packaging/coating material, to enhance food safety and extend the food shelf-life. Nevertheless, the required final concentration of active compounds in the film must be fitted, taking into account the MIC values for a target microorganism and the release kinetics of active from the matrix to the food surface. Thus, further studies are needed to investigate potential performance improvement for specific food applications.

**Acknowledgments** This work was financially supported by the Project PICT 2011-1213 (ANPCyT, Argentina) and Project AGL2013-42989-R (Ministerio de Economía y Competitividad, España). M. J. Bof acknowledges to the Argentinean Scholarship Program for Professionals Abroad (Bec.ar).

## Compliance with Ethical Statement

**Conflict of interest** The authors have declare that they have no conflicts of interest.

**Funding** The present work was financially supported by CONICET Argentina, UNLP, and ANPCyT (Project PICT 2011-1213).

## References

- AL-Jabri, N. N., & Hossain, M. A. (2014). Comparative chemical composition and antimicrobial activity study of essential oils from two imported lemon fruits samples against pathogenic bacteria. *Benisuef University Journal of Basic and Applied Sciences*, 3(4), 247–253.
- ASTM (1995). Standard test methods for water vapour transmission of materials. Standards Designations: E96–95. In *Annual book of ASTM standards* (pp. 406–413). Philadelphia, PA: American Society for Testing and Materials.

- ASTM (1999). Standard test method for specular gloss. Designation (D523). Annual book of ASTM standards, Vol. 06.01 American Society for Testing and Materials, Philadelphia, PA.
- ASTM (2001). Standard test method for tensile properties of thin plastic sheeting. Standard D882. Annual book of American standard testing methods. American Society for Testing and Materials, Philadelphia, PA.
- Bertuzzi, M. A., Castro Vidaurre, E. F., Armada, M., & Gottifredi, J. C. (2007). Water vapor permeability of edible starch based films. *Journal of Food Engineering*, *80*(3), 972–978.
- Bof, M. J., García, M. A., Locaso, D., & Zambón, Y. (2014). Películas compuestas a base de almidón y quitosano: formulación y caracterización. In Proceedings of the International Conference on Food Innovation. Food Innova 2014 (3rd ed.). (p. 148). Concepción del Uruguay: Universidad Nacional de Entre Ríos.
- Bof, M. J., Bordagaray, V. C., Locaso, D. E., & García, M. A. (2015). Chitosan molecular weight effect on starch-composite film properties. *Food Hydrocolloids*, *51*, 281–294.
- Bonilla, J., Vargas, M., Atarés, L., & Chiralt, A. (2011). Physical properties of chitosan-basil essential oil edible films as affected by oil content and homogenization conditions. *Procedia Food Science*, *1*, 50–56.
- Bonilla, J., Atarés, L., Vargas, M., & Chiralt, A. (2013). Properties of wheat starch film-forming dispersions and films as affected by chitosan addition. *Journal of Food Engineering*, *114*(3), 303–312.
- Boumail, A., Salmieri, S., Klimas, E., Tawema, P. O., Bouchard, J., & Lacroix, M. (2013). Characterization of trilayer antimicrobial diffusion films (ADFs) based on methylcellulose–polycaprolactone composites. *Journal of Agricultural Food and Chemistry*, *61*(4), 811–821.
- De Campos, A., Teodoro, K. B. R., Marconcini, J. M., & Mattoso, L. H. C. (2011). Effect of fiber treatments on properties of thermoplastic starch/polycaprolactone/sisal biocomposites. *Polymers*, *21*(3), 217–222.
- Duarte, M. L., Ferreira, M. C., Marvao, M. R., & Rocha, J. (2002). An optimised method to determine the degree of acetylation of chitin and chitosan by FTIR spectroscopy. *International Journal of Biological Macromolecules*, *31*(1–3), 1–8.
- García, M. A., Pinotti, A., & Zaritzky, N. E. (2006). Physicochemical, water vapor barrier and mechanical properties of corn starch and chitosan composite films. *Starch/Stärke*, *58*(9), 453–463.
- García, N. L., Fama, L., Dufresne, A., Aranguren, M., & Goyanes, S. (2009). A comparison between the physico-chemical properties of tuber and cereal starches. *Food Research International*, *42*, 976–982.
- Ghasemlou, M., Aliheidaric, N., Fahmid, R., Shojaee-Aliabadie, S., Keshavarzf, B., Crang, M. J., & Khaksare, R. (2013). Physical, mechanical and barrier properties of corn starch films incorporated with plant essential oils. *Carbohydrate Polymers*, *98*(1), 1117–1126.
- Han, J. H. (2014). Edible films and coatings: a review. In J. H. Han (Ed.), *Innovations in food packaging* (pp. 240–255). London: Elsevier.
- Hong, Y. H., Lim, G. O., & Song, K. B. (2009). Physical properties of *Gelidium corneum* gelatin blends films containing grapefruit seed extract or green tea extract and its application in the packaging of pork loins. *Journal of Food Science*, *74*(1), C6–C10.
- Hosseini, S. F., Rezaei, M., Zandi, M., & Farahmandghavi, F. (2016). Development of bioactive fish gelatin/chitosan nanoparticles composite films with antimicrobial properties. *Food Chemistry*, *194*(1), 1266–1274.
- Jang, S. A., Shin, Y. J., & Song, K. B. (2011). Effects of rapeseed protein-gelatin film containing grapefruit seed extract on 'Machyang' strawberry quality. *International Journal of Food Science and Technology*, *46*(3), 620–625.
- Jiménez, A., Fabra, M. J., Talens, P., & Chiralt, A. (2012). Effect of recrystallization on tensile, optical and water vapour barrier properties of corn starch films containing fatty acids. *Food Hydrocolloids*, *26*(1), 302–310.
- Jiménez, A., Fabra, M. J., Talens, P., & Chiralt, A. (2013a). Physical properties and antioxidant capacity of starch-sodium caseinate films containing lipids. *Journal of Food Engineering*, *116*(3), 695–702.
- Jiménez, A., Fabra, M. J., Talens, P., & Chiralt, A. (2013b). Phase transitions in starch based films containing fatty acids. Effect on water sorption and mechanical behavior. *Food Hydrocolloids*, *30*(1), 408–418.
- Jiménez, A., Sánchez-González, L., Desobry, S., Chiralt, A., & Tehrani, E. A. (2014). Influence of nanoliposomes incorporation on properties of film forming dispersions and films based on corn starch and sodium caseinate. *Food Hydrocolloids*, *35*, 159–169.
- Kanmani, P., & Rhim, J.-W. (2014). Antimicrobial and physical-mechanical properties of agar-based films incorporated with grapefruit seed extract. *Carbohydrate Polymers*, *102*, 708–716.
- Kavoosi, G., Dadfar, S. M. M., & Purfard, A. M. (2013). Mechanical, physical, antioxidant, and antimicrobial properties of gelatin films incorporated with thymol for potential use as nano wound dressing. *Journal of Food Science*, *78*(2), 244–250.
- Lim, G. O., Jang, S. A., & Song, K. B. (2010). Physical and antimicrobial properties of *Gelidium corneum*/nano-clay composite film containing grapefruit seed extract and thymol. *Journal of Food Engineering*, *98*(4), 415–420.
- Liu, H., Du, Y., Wang, X., & Sun, L. (2002). Chitosan kills bacteria through cell membrane damage. *International Journal of Food Microbiology*, *95*(2), 147–155.
- Luo, X., Li, J., & Lin, X. (2012). Effect of gelatinization and additives on morphology and thermal behavior of comstarch/PVA blend films. *Carbohydrate Polymers*, *90*(4), 1595–1600.
- Martínez-Camacho, A. P., Cortez-Rocha, M. O., Ezquerro-Brauer, J. M., Graciano-Verdugo, A. Z., Rodríguez-Félix, F., Castillo-Ortega, M. M., Yépiz-Gómez, M. S., & Plascencia-Jatomea, M. (2010). Chitosan composite films: thermal, structural, mechanical and antifungal properties. *Carbohydrate Polymers*, *82*(2), 305–315.
- Mc Hugh, T. H., Avena-Bustillos, R., & Krochta, J. M. (1993). Hydrophobic edible films: modified procedure for water vapor permeability and explanation of thickness effects. *Journal of Food Science*, *58*(4), 899–903.
- Mei, J., Yuan, Y., Wu, Y., & Li, Y. (2013). Characterization of edible starch–chitosan film and its application in the storage of Mongolian cheese. *International Journal of Biological Macromolecules*, *57*, 17–21.
- No, H. K., Park, N. Y., Lee, S. H., & Meyers, S. P. (2002). Antibacterial activity of chitosans and chitosan oligomers with different molecular weights. *International Journal of Food Microbiology*, *74*(1–2), 65–72.
- Ortega-Toro, R., Jiménez, A., Talens, P., & Chiralt, A. (2014). Effect of the incorporation of surfactants on the physical properties of corn starch films. *Food Hydrocolloids*, *38*, 66–75.
- Ortega-Toro, R., Collazo-Bigliardi, S., Talens, P., & Chiralt, A. (2015). Influence of citric acid on the properties and stability of starch-polycaprolactone based films. *Journal of Applied Polymer Science*, *133*, 42220. doi:10.1002/app.42220.
- Perdones, A., Sánchez-González, L., Chiralt, A., & Vargas, M. (2012). Effect of chitosan-lemon essential oil coatings on storage-keeping quality of strawberry. *Postharvest Biology and Technology*, *70*, 32–41.
- Re, R., Pellegrini, N., Proteggente, A., Pannala, A., Yang, M., & Rice-Evans, C. (1999). Antioxidant activity applying an improved ABTS radical cation decolorization assay. *Free Radical Biology & Medicine*, *26*(9–10), 1231–1237.
- Rivero, S., García, M. A., & Pinotti, A. (2010). Crosslinking capacity of tannic acid in plasticized chitosan films. *Carbohydrate Polymers*, *82*(2), 270–276.
- Sánchez Aldana, D., Contreras-Esquiveola, J. C., Nevárez-Moorillón, G. V., & Aguilar, C. N. (2014). Caracterización de películas



- comestibles a base de extractos pécticos y aceite esencial de limón Mexicano. *CyTA - Journal of Food*, 12, 1–9.
- Sanchez-Gonzalez, L., Cháfer, M., Chiralt, A., & Gonzalez-Martínez, C. (2010). Physical properties of edible chitosan films containing bergamot essential oil and their inhibitory action on *Penicillium italicum*. *Carbohydrate Polymers*, 82(2), 277–283.
- Song, H. Y., Shin, Y. J., & Song, K. B. (2012). Preparation of a barley bran protein–gelatin composite film containing grapefruit seed extract and its application in salmon packaging. *Journal of Food Engineering*, 113(4), 541–547.
- Teixeira, B., Marques, A., Ramos, C., Neng, N. R., Nogueira, J. M. F., Saraiva, J. A., & Nunes, M. L. (2013). Chemical composition and antibacterial and antioxidant properties of commercial essential oils. *Industrial Crops and Products*, 43, 587–595.
- Tepe, B., Sokmen, M., Sokmen, A., Daferera, D., & Polissiou, M. (2005). Antimicrobial and antioxidative activity of the essential oil and various extracts of *Cyclotrichium origanifolium* (Labill) Manden & Scheng. *Journal of Food Engineering*, 69(3), 335–342.
- Tongnuanchan, P., Benjakul, S., & Prodpran, S. (2012). Properties and antioxidant activity of fish skin gelatin film incorporated with citrus essential oils. *Food Chemistry*, 134(3), 1571–1579.
- Tsai, G.-J., Su, W.-H., Chen, H.-C., & Pan, C.-L. (2002). Antimicrobial activity of shrimp chitin and chitosan from different treatments and applications of fish preservation. *Fisheries Science*, 68(1), 170–177.
- Vargas, M., Sánchez-González, L., Cháfer, M., Chiralt, A., & González-Martínez, C. (2012). Edible chitosan coatings for fresh and minimally processed foods. In K. L. Yam & D. S. Lee (Eds.), *Emerging food packaging technologies: principles and practice* (pp. 66–95). Oxford, Philadelphia, PA: Woodhead Publishing.
- Villalobos, R., Chanona, J., Hernández, P., Gutiérrez, G., & Chiralt, A. (2005). Gloss and transparency of hydroxypropyl methylcellulose films containing surfactants as affected by their microstructure. *Food Hydrocolloids*, 19(1), 53–61.
- Viuda-Martos, M., Ruiz-Navajas, Y., Fernandez-Lopez, J., & Perez-Alvarez, J. (2008). Antifungal activity of lemon (*Citrus lemon* L.), mandarin (*Citrus reticulata* L.), grapefruit (*Citrus paradisi* L.) and orange (*Citrus sinensis* L.) essential oils. *Journal of Food Control*, 19(12), 1130–1138.
- Wilhelm, H., Sierakowski, M., Souza, G. & Wypych, F. (2003). Starch films reinforced with mineral clay. *Carbohydrate Polymers*, 52, 101–110.
- Xu, W., Qu, W., Huang, K., Guo, F., Yang, J., Zhao, H., & Luo, Y.-B. (2007a). Antibacterial effect of grapefruit seed extract on food-borne pathogens and its application in the preservation of minimally processed vegetables. *Postharvest Biology and Technology*, 45(1), 126–133.
- Xu, W.-T., Huang, K.-L., Guo, F., Qu, W., Yang, J.-J., Liang, Z.-H., & Luo, Y.-B. (2007b). Postharvest grapefruit seed extract and chitosan treatments of table-grapes to control *Botrytis cinerea*. *Postharvest Biology and Technology*, 46(1), 86–94.
- Zhang, H. Y., Arab Tehrani, E., Kahn, C. J. F., Ponçot, M., Linder, M., & Cleymand, F. (2012). Effects of nanoliposomes based on soya, rapeseed and fish lecithins on chitosan thin films designed for tissue engineering. *Carbohydrate Polymers*, 88(2), 618–627.